Neutron irradiation effects in different tungsten microstructures

D. Papadakis[a,b], S. Dellis[a], V. Chatzikos[a,c], E.Manios[a], I.E.Stamatelatos[a], S. Messoloras[a] and K. Mergia[a,*]

[a] *Institute of Nuclear and Radiological Sciences and Technology, Energy and Safety, NCSR Demokritos, Athens, 15310, Greece*

[b] *Department of Physics, School of Sciences, University of Athens, Athens, 15772, Greece*

[c] *Department of Physics, School of Sciences, University of Ioannina, Ioannina, 45110, Greece*

Abstract

In this work the relation of the neutron irradiation induced damage and the initial material microstructure is investigated. Further the modification of the structure as the result of the neutron irradiation is accessed and its effects on the mechanical properties is determined. Forged bar (ITER grade), cold rolled sheet and single crystalline tungsten materials were neutron irradiated at 600 °C to a damage of 0.12 displacements per atom. Positron annihilation lifetime spectroscopy reveals the formation of voids of about the same size in all tungsten grades after neutron irradiation. From the radiation induced electrical resistivity the total dislocation line density is determined. Irradiation hardening is observed, 13% for the cold rolled sheet, 29% for the forged bar and 47% for the single crystal. The yield strength of the polycrystalline materials presents similar increase with that of hardness demonstrating the correlation between the two properties.

* Corresponding author K. Mergia, email: kmergia@ipta.demokritos.gr

1 Introduction

Tungsten (W) presents significant advantageous properties for its application in plasma facing components (PFCs) in fusion reactors [1]. However, for the use of W as a PFC its inherent brittleness should be overcome. To that end microstructural modification processes have been proposed [2] for the reduction of its brittle to ductile transition temperature (BDTT) and increase of its strength, with cold rolling [3,4] and forging [5] providing promising results.

For the application of W in PFCs in-depth understanding of the neutron irradiation induced microstructural changes and their effects on its mechanical properties are required. The use of fission neutrons to simulate the neutron irradiation conditions in a fusion reactor is the most common approach [6–8]. The radiation induced damage refers mainly to the formation of vacancy clusters or voids, dislocations loops [9–11] and transmutation products [12–14], while the type and population of the induced defects are dictated by the neutron irradiation conditions [8,15,16].

In the current work we investigate the influence of the tungsten initial microstructure on the neutron induced irradiation damage and the effect of the latter on its mechanical properties. The neutron induced defects were studied using positron annihilation lifetime spectroscopy (PALS) and electrical resistivity measurements and the mechanical properties were assessed employing depth sensing indentation (DSI). Three W grades, namely, W(100) single crystal, ITER grade forged bar and cold rolled sheet irradiated at 600 °C to 0.12 displacements per atom (dpa) were investigated.

2 Materials and Methods

2.1 Materials and Irradiation

The production route of the W polycrystalline materials used in the current study and their reference microstructure are presented in Ref [17–19]. The W(100) single crystal (SC) of 99.999 % purity was supplied by MaTeck. Disks with a diameter of about 11 mm were sectioned from the three W materials and were polished to obtain mirror quality surface as described in [19]. The final thickness of the samples was about 0.5 mm.

Neutron irradiations were performed at the Belgian Material Test Reactor BR2, and the details of the irradiation conditions are presented in Ref. [20]. The irradiation dose was calculated to 0.12 dpa based on the total fast neutron fluence (5.8×10^{20} n/cm^2, >0.1 MeV) achieved after an irradiation period of 49 days. The concentration of the transmutation products according to nuclide inventory calculations using FISPACT-II code and TENDL-17 nuclear database was found 0.37 at% Re, 6×10^{-3} at% Os and 5.7×10^{-3} at% Ta.

2.1 Positron Annihilation Lifetime Spectroscopy (PALS)

PALS measurements were performed at room temperature using the Ortec® PLS-system employing two plastic scintillation detectors. The details regarding the PALS methodology and the analysis of the spectra are presented in Ref [21].

2.2 Resistivity

Electrical resistivity measurements were carried out employing the collinear 4-point probe (4PP) method using Keithley 2182A nanovoltmeter and Keithley 6221 AC and DC current source. The details of the measurements are presented in Ref [21].

2.3 Mechanical Properties

2.3.1 Vickers Hardness

Microindentation experiments were performed using a Vickers indenter to asses the materials' Vickers hardness, H_V, employing NANOVEA's mechanical tester. In each specimen nine tests were made with a maximum applied load of 3 N and a loading/unloading rate of 20 N/min. A holding time of 200 s was applied before the start of the unloading process. The H_V was calculated as the ratio of the maximum applied load to the contact area. For the measurement of the hardness of the W(100) SC specimens the dependence on the orientation of the Vickers indenter with respect to the crystallographic axes was considered and the mean hardness was determined [20].

2.3.2 Stress-Strain curves

For the determination of the true stress-strain, $\sigma_{tr} - \varepsilon_{tr}$, curves a spherical indenter of 200 μm radius, a maximum applied load of 100 N, and a loading/unloading rate of 20 N/min were employed using NANOVEA's mechanical tester. Initially, the indentation strain, ε_{ind}, and stress, σ_{ind}, were determined through the relations

$$\begin{aligned} \varepsilon_{ind} &= R_c / R_{ind} \\ \sigma_{ind} &= F / \pi R_c^2 \end{aligned}, \qquad (1)$$

where R_{ind} is the indenter radius and R_c is the contact radius calculated as

$$R_c = \sqrt{2 R_{ind} h - h^2}\,, \qquad (2)$$

where h is the penetration depth at the applied load F. Then the indentation stress-strain curves, $\sigma_{ind} - \varepsilon_{ind}$, were transformed to true stress-strain curves, $\sigma_{tr} - \varepsilon_{tr}$ using the ϕ and ψ strain and stress constraint factors, respectively, as

$$\varepsilon_{tr} = \phi\varepsilon_{ind}$$
$$\sigma_{tr} = \sigma_{ind} / \psi, \quad (3)$$

The ϕ and ψ constraint factors were determined by the scaling of the indentation stress-strain curves of the unirradiated cold rolled W plate and W SC to coincide with the stress-strain curves of the same type of W materials from conventional tensile tests [22,23]. The ψ and ϕ factors were determined 2.1 and 0.1 for the plate, and 4.2 and 0.2 and the SC, respectively. These constrain factors are close to those reported in the literature (2-3 for ψ and 0.1-0.32 for ϕ) [24–29]. The constrain factors derived for the unirradiated plate were also used for the determination of the stress-strain curves of the bar. The yield strength, YS, was determined at the constant strain of 1%.

3 Results

3.1 Positron Annihilation Spectroscopy (PAS)

From the PALS spectra the positron lifetimes in the defects present in the material are determined. For the unirradiated W SC a single lifetime, τ_0, was needed to describe the PALS spectrum and it was found (114±1) ps (Figure 1a), a value which is in the range of positron lifetimes (100-116 ps) reported in the literature for defect free tungsten [30–36]. This finding leads to the conclusion that, as expected, the W SC material is defect free. In contrast, for the unirradiated W plate and bar materials an additional lifetime, τ_1, was needed for the description of the PALS spectra. Its value was found (171±16) ps for the plate and (185±8) ps for the bar with a relative intensity, I_1, of (75±16)% and (45±3)% (Figure 1b), respectively. The lifetimes for mono-vacancy and dislocation defects are reported in the range of 160-200 ps and 130–180 ps, respectively [32,33,37–39]. Also, the positron lifetime of a vacancy associated to either screw or edge dislocation was calculated in the range from 188 to 192 ps [35]. Therefore, the lifetime τ_1 of the unirradiated plate and bar is attributed to positron annihilations mainly in dislocations. The plate material presents a larger relative intensity, I_1, (Figure 1b) which indicates that the number density of dislocations in the plate material is larger than that in the bar, as it is expected since the induced deformation is larger in the cold rolling fabrication process compared to forging. This finding is in agreement with TEM results [8], which show larger dislocation density for the unirradiated cold rolled plate compared to the forged bar.

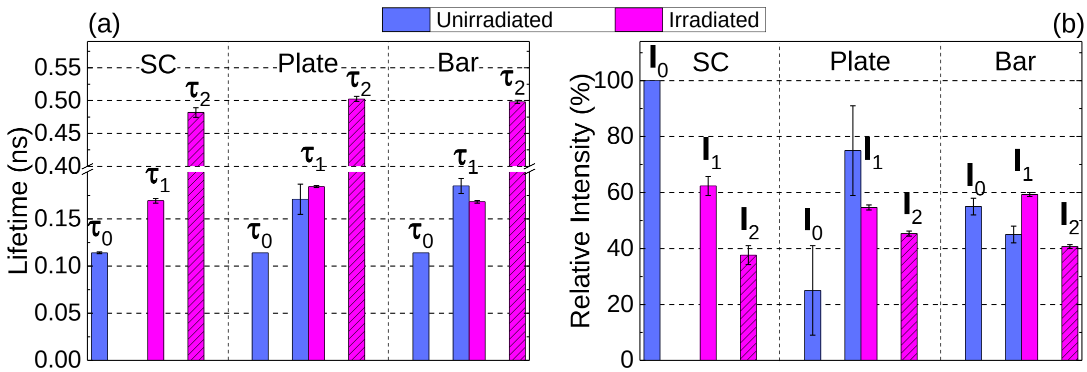

Figure 1. Positron lifetimes (a) and relative intensities (b) for the unirradiated and irradiated at 600 °C to 0.12 dpa W SC, plate and bar.

Two lifetimes, τ_1 and τ_2, were required to fit the PALS spectra of all the irradiated specimens. The short lifetime, τ_1, presents a value in the range from 165 to 185 ps (Figure 1a), which according to the discussion above is attributed to positron annihilations mainly in dislocations. The τ_1 lifetimes for the SC ((169±3) ps) and bar ((168±1) ps) are almost equal whereas for the plate τ_1 is slightly higher of (184±1) ps. The relative intensities, I_1, corresponding to τ_1 lifetime for the three materials (Figure 1b) are very close indicating that the number of the dislocations at the end of the irradiation is material microstructure independent. According to the electrical resistivity results (discussed below), the dislocation number density does not change significantly among the three irradiated W materials. This conclusion is in agreement with TEM findings [8].

The long lifetime, τ_2, is found in the range from 482 to 503 ps for all the W materials, (482±7) ps for the SC, (503±4) ps for the plate and (498±3) ps for bar (Figure 1a). According to [34,40] τ_2 is associated with large vacancy clusters containing more than 40 vacancies. Thus, it is concluded that neutron irradiation at the temperature of 600 °C results in the formation of voids with similar size (>1 nm) for all tungsten grades. The relative intensity, I_2, represents the percentage of positrons annihilating in the voids. The SC and bar materials exhibit similar I_2 values of (38±3)% and (40.7±0.7)% respectively, smaller than that found for the plate being of (45.3±0.9)% (Figure 1b). Thus it can be concluded that the void number density for the SC and bar material is similar, while for the plate material is higher. This is also confirmed by TEM measurements of the three W grades irradiated at the same temperature to a similar dose of 0.18 dpa [8].

3.2 Electrical Resistivity

The electrical resistivity, ρ, of the unirradiated SC is (5.46±0.03) μΩ·cm, while that of the unirradiated bar and the plate is higher and of the same value ((5.65±0.05) μΩ·cm). The difference in ρ between the SC and the polycrystalline materials arises from electron scattering from dislocations and grain boundaries originating from the fabrication process. The resistivity of the irradiated samples was found larger than that of the unirradiated ones (Figure 2) reflecting the additional electron scattering from the irradiation induced defects and transmutation products. By subtracting the resistivity of the unirradiated sample from that of the irradiated samples the Radiation Induced Resistivity, RIR, is derived. With this subtraction the electrical resistivity arising from the scattering of conduction electrons from phonons and also scattering arising from dislocations or other defects produced during the fabrication process of the material have been removed. RIR can be considered as the sum of three main components (ignoring cross scattering of the electrons from the different defects) [21]

$$RIR = RIR_{void} + RIR_{disl} + RIR_{trans} \tag{4}$$

where RIR_{void}, RIR_{disl} and RIR_{trans} are the contributions of voids (including mono- or clusters of vacancies), dislocation loops and lines and transmutation products, respectively. The methodology for calculating each contributing component is described in [21].

The increase in resistivity, RIR, after irradiation is similar for all W grades (Figure 2). Regarding the transmutation products, the calculated concentration for Os and Ta are about two orders of magnitude lower than that of Re and therefore only Re is taken into account for the calculation of RIR_{trans}. RIR_{trans} is found equal to (0.49±0.02) μΩ·cm. An upper limit for the voids contribution, RIR_{void}^{max}, can be estimated employing TEM results for the void size and their number density of the same materials irradiated to a similar dose (0.18 dpa). This is found equal to 0.02 μΩ·cm which is negligible compared to the total RIR. Therefore from eq.(4) as $RIR_{void} \approx 0$ and using the calculated value for RIR_{trans} we can obtain the RIR_{disl}, From RIR_{disl} the total dislocation line density, N_{disl}, can be determined using for the dislocation specific resistivity the value of $2.6 \times 10^{-23}\ \Omega \cdot \mathrm{m}^3$ [21]. The determined values for N_{disl} are depicted in Figure 2 and they are (1.8±0.3)×10^{14} m^{-2} for the SC, (2.4±0.3)×10^{14} m^{-2} for the plate and (1.6±0.3)×10^{14} m^{-2} for the bar. These results are in very good agreement with those obtained from the TEM investigation in [8].

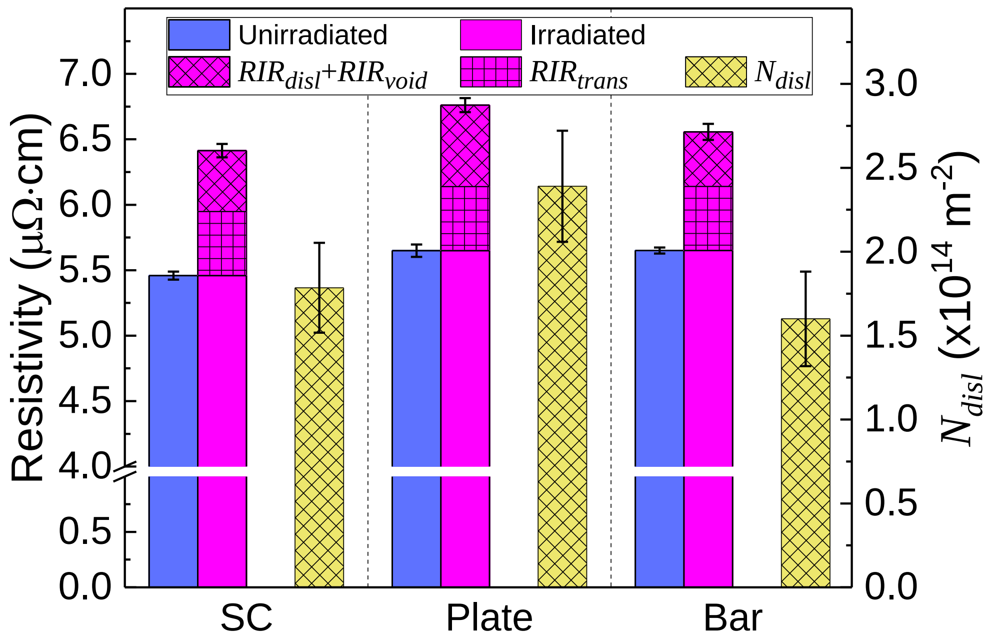

Figure 2. Resistivity of unirradiated and irradiated tungsten SC, plate and bar, showing the contributions of $RIR_{void} + RIR_{disl}$ and RIR_{trans}. The total dislocation line density, N_{disl}, after irradiation is also presented (see text for details).

3.3 Mechanical Properties

Irradiation results in the Vickers hardness (H_V) increase of all W materials. The H_V of the SC exhibits the highest hardening of (47.0 ± 0.1)% whereas the polycrystalline specimens exhibit significantly lower hardening of (29 ± 3)% and (13 ± 2)% for the bar and plate, respectively (figure 3a). The lower hardening of the polycrystalline specimens is attributed to their high degree of deformation leading to the creation of fine-grains and a relatively high dislocation density. Indeed, the plate, which has been through the highest deformation, presents the lowest hardening.

The stress-strain curves (Figure 3b) after irradiation show a strengthening effect which is more profound in SC. The slope of the elastic region at the beginning of the stress-strain curve, which defines the elastic modulus E, was determined by impulse excitation measurements (not presented). The yield strength, YS, of the SC, bar and plate increases after irradiation by (25±2)%, (15±2)% and (6±2)%, respectively. For the polycrystalline W materials the relation $H_V = 3 \cdot YS$, established by Tabor [41], is a good approximation both before and after irradiation with the ratio $k = H_V / YS$ slightly increasing after irradiation (Figure 3a). In the case of the SC k increases after irradiation, from 6.68±0.08 to7.87±0.05, being significantly higher than 3. The deviation of k from the value of 3 for the SC is expected as the relation $H_V = 3 \cdot YS$ is valid for perfect plastic materials that do not present work hardening. This condition is fulfilled for the polycrystalline materials that have sustained high deformation. The ultimate tensile strength, UTS, for the unirradiated W SC is in the range 0.9 and 0.96 GPa [42]. If we use the UTS value instead of the YS one for the calculation of the ratio k then k is found in the range 3.5-3.8, indicating that the H_V of the SC should not be correlated with its YS but with its ultimate tensile stress [43].

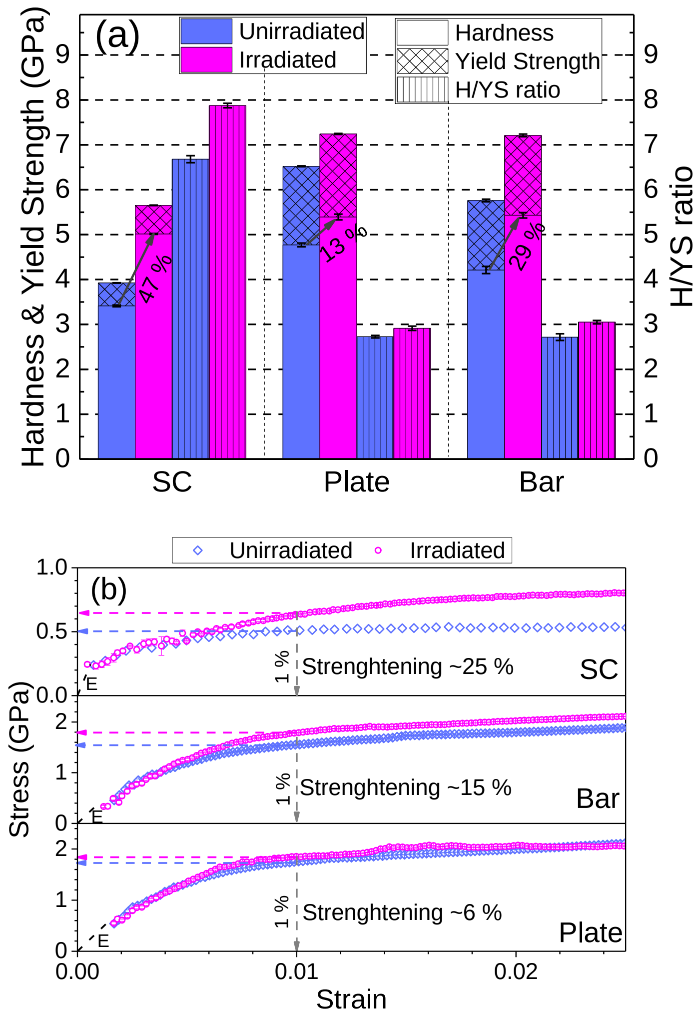

Figure 3. (a) Vickers hardness, yield strength and their ratio, of unirradiated and irradiated W SC, plate, and bar. (b) True stress-strain curves before and after irradiation of SC, plate and bar. The % increase of the yield strength (strengthening) at a strain of 1% is depicted.

4 Summary and Conclusions

Three W material grades, single crystal, cold rolled plate and forged bar, have been irradiated at 600 °C to 0.12 dpa. According to PALS results the unirradiated SC material is defect free, whereas dislocations are present in the polycrystalline W materials due to their fabrication process. The dislocation density of the unirradiated plate is higher than that in the bar. After irradiation at 600 °C PALS shows the formation of dislocations both in the SC and the bar materials as well as the formation of voids containing more than 40 vacancies and having a size larger than 1 nm in all W materials. The void and total dislocation density is similar in all irradiated W materials with the dislocation density being in the range $(1.6\text{-}2.4)\times10^{14}$ m^{-2}. Irradiation results in the increase of the hardness and yield strength of all W grades. The hardening and strengthening of the materials are highly influenced by their initial microstructure; the deformation of the polycrystalline material results into significantly reduced hardening and strengthening compared to the single crystalline material. The higher the initial deformation is, the lower the hardening/strengthening of the material. Additionally, hardness can offer a measure of the yield strength of the polycrystalline material as the proportionality constant of about three between hardness and yield strength applies for both unirradiated and irradiated W materials.

Acknowledgments

This work has been carried out within the framework of the EUROfusion Consortium and has received funding from the Euratom research and training programme 2014-2018 and 2019-2020 under grant agreement No 633053. The views and opinions expressed herein do not necessarily reflect those of the European Commission.

We thank Dr M. Rieth from Karlsruhe Institute of Technology and Dr G. Pintsuk from Forschungszentrum Jülich GmbH for the provision of the tungsten cold rolled plate and forged bar material, respectively.

References

[1] Pintsuk G 2012 vol 4 (Elsevier Inc.)

[2] Ren C, Fang Z Z, Xu L, Ligda J P, Paramore J D and Butler B G 2019 *Acta Mater.* **162** 202–13

[3] Reiser J, Hoffmann J, Jäntsch U, Klimenkov M, Bonk S, Bonnekoh C, Rieth M, Hoffmann A and Mrotzek T 2016 *Int. J. Refract. Met. Hard Mater.* **54** 351–69

[4] Bonnekoh C, Hoffmann A and Reiser J 2018 *Int. J. Refract. Met. Hard Mater.* **71** 181–9

[5] Yin C, Terentyev D, Pardoen T, Bakaeva A, Petrov R, Antusch S, Rieth M, Vilémová M, Matějíček J and Zhang T 2018 *Int. J. Refract. Met. Hard Mater.* **75** 153–62

[6] Rieth M, Doerner R, Hasegawa A, Ueda Y and Wirtz M 2019 *J. Nucl. Mater.* **519** 334–68

[7] Hasegawa A, Fukuda M, Yabuuchi K and Nogami S 2016 *J. Nucl. Mater.* **471** 175–83

[8] Dubinko A, Terentyev D, Yin C, Van Renterghem W, Rossaert B, Rieth M, Zhurkin E E, Zinovev A, Chang C C, Van Dyck S and Bonny G 2021 *Int. J. Refract. Met. Hard Mater.* **98** 105522

[9] Brinkman J A 1954 *J. Appl. Phys.* **25** 961–70

[10] Buswell J T 1970 *Philos. Mag.* **22** 787–802

[11] Rau R C, Ladd R L and Moteff J 1969 *J. Nucl. Mater.* **33** 324–7

[12] Klimenkov M, Jäntsch U, Rieth M, Schneider H C, Armstrong D E J, Gibson J and Roberts S G 2016 *Nucl. Mater. Energy* **9** 480–3

[13] Lloyd M J, Abernethy R G, Gilbert M R, Griffiths I, Bagot P A J, Nguyen-Manh D, Moody M P and Armstrong D E J 2019 *Scr. Mater.* **173** 96–100

[14] Gilbert M R and Sublet J C 2011 *Nucl. Fusion* **51**

[15] Hasegawa A, Fukuda M, Nogami S and Yabuuchi K 2014 *Fusion Eng. Des.* **89** 1568–72

[16] Katoh Y, Snead L L, Garrison L M, Hu X, Koyanagi T, Parish C M, Edmondson P D, Fukuda M, Hwang T, Tanaka T and Hasegawa A 2019 *J. Nucl. Mater.* **520** 193–207

[17] Krimpalis S, Mergia K, Messoloras S, Dubinko A, Terentyev D, Triantou K, Reiser J and Pintsuk G 2017 *Phys. Scr.* **T170** 014068

[18] Wirtz M, Uytdenhouwen I, Barabash V, Escourbiac F, Hirai T, Linke J, Loewenhoff T, Panayotis S and Pintsuk G 2017 *Nucl. Fusion* **57** 066018

[19] Papadakis D, Dellis S, Mergia K, Chatzikos V, Terentyev D, Bonny G, Dubinko A, Renterghem W Van, Konstantinovic M, Messoloras S and Pintsuk G 2021 *Fusion Eng. Des.* **168** 112608

[20] Dellis S, Xiao X, Terentyev D, Mergia K and Krimpalis S *J. Nucl. Mater.* 1–30

[21] Mergia K, Chatzikos V, Manios E, Dellis S, Papadakis D, Terentyev D, Bonny G, Dubinko A, Stamatelatos I E and Messoloras S *Fusion Eng. Des.*(submitted, under minor revision)

[22] Bonk S, Hoffmann J, Hoffmann A and Reiser J 2018 *Int. J. Refract. Met. Hard Mater.* **70** 124–33

[23] Argon A . and Maloof S . 1966 *Acta Metall.* **14** 1449–62

[24] Herbert E ., Pharr G ., Oliver W ., Lucas B . and Hay J . 2001 *Thin Solid Films* **398**–**399** 331–5

[25] Tirupataiah Y and Sundararajan G 1991 *Metall. Trans. A* **22** 2375–84

[26] Jeon E C, Kim J Y, Baik M K, Kim S H, Park J S and Kwon D 2006 *Mater. Sci. Eng. A* **419** 196–201

[27] Pathak S, Shaffer J and Kalidindi S R 2009 *Scr. Mater.* **60** 439–42

[28] Patel D K and Kalidindi S R 2016 *Acta Mater.* **112** 295–302

[29] Chang C, Garrido M A, Ruiz-Hervias J, Zhang Z and Zhang L 2018 *Adv. Mater. Sci. Eng.* **2018** 1–9

[30] Campillo Robles J M and Plazaola F 2003 *Defect Diffus. Forum* **213**–**215** 141–236

[31] Puska M J 1991 *J. Phys. Condens. Matter* **3** 3455–69

[32] Staab T E M, Krause-Rehberg R, Vetter B and Kieback B 1999 *J. Phys. Condens. Matter* **11** 1757–86

[33] Zhu S, Xu Y, Wang Z, Zheng Y, Zhou D, Du E, Yuan D, Fukuda M, Mihara M, Matsuta K and Minamisono T 2005 *J. Nucl. Mater.* **343** 330–2

[34] Troev T, Popov E, Nankov N and Yoshiie T 2010 *J. Phys. Conf. Ser.* **207** 012033

[35] Staikov P and Djourelov N 2013 *Phys. B Condens. Matter* **413** 59–63

[36] Heikinheimo J, Mizohata K, Räisänen J, Ahlgren T, Jalkanen P, Lahtinen A, Catarino N, Alves E and Tuomisto F 2019 *APL Mater.* **7**

[37] Ogorodnikova O V., Majerle M, Gann V V., Čížek J, Hruška P, Simakov S, Štefánik M and Zach V 2019 *J. Nucl. Mater.* **525** 22–31

[38] Lhuillier P E, Barthe M F, Desgardin P, Egger W and Sperr P 2009 *Phys. status solidi* **6** 2329–32

[39] Yabuuchi A, Tanaka M and Kinomura A 2020 *J. Nucl. Mater.* **542**

[40] Hu X, Koyanagi T, Fukuda M, Katoh Y, Snead L L and Wirth B D 2016 *J. Nucl. Mater.* **470** 278–89

[41] Tabor D 1956 *Br. J. Appl. Phys.* **7** 159–66

[42] Lassner E and Schubert W-D 1999 (Boston, MA: Springer US)

[43] Zhang P, Li S X and Zhang Z F 2011 *Mater. Sci. Eng. A* **529** 62–73